International Journal of Emerging Research in Engineering, Science, and Management
Vol. 5 | Issue 3 | pp. 81-96 | Jul-Sep 2026.
www.ijeresm.com | eISSN – 2583-4894
Received: 27 Apr 2026 | Revised: 29 Jul 2026 | Accepted: 12 Aug 2026 | Published: 30 Aug 2026

Multipath-Aware Hybrid Adaptive Wavelet Thresholding for Denoising Underwater Acoustic BPSK Communication Signals

[1]B. Shiny, [2]Vijayalakshmi P, [3]M. Monisha, [4]Rajendran V

Department of Electronics and Communication Engineering,
Vels Institute of Science, Technology, and Advanced Studies (VISTAS), Chennai, India
[1]flawsomeshiny03@gmail.com, ORCID ID: 0009-0000-7480-2223
[2]viji.se@vistas.ac.in, ORCID ID: 0000-0002-7339-857X
[3]monisha.se@vistas.ac.in, ORCID ID: 0000-0003-4794-5565
[4]director.ece@vistas.ac.in, ORCID ID: 0000-0002-6819-3991

**Corresponding Author: Vijayalakshmi P*

Abstract: This paper presents a hybrid adaptive wavelet thresholding method for denoising underwater multipath Binary Phase Shift Keying (BPSK) communication signals corrupted by real ambient noise. A raised-cosine pulse-shaped BPSK signal is transmitted through simulated underwater acoustic channels with varying delay spreads and channel conditions to model realistic underwater propagation. Real ambient underwater noise is added to the transmitted signal at input SNRs of -15, −10, −5, 0, and 5 dB to evaluate the proposed method's robustness under different noise levels. The noisy signal is decomposed using the Continuous Wavelet Transform (CWT) with the Analytic Morlet wavelet. The proposed hybrid method combines adaptive covariance-based weighting with soft thresholding to preserve the transient burst features. Delay-dependent correlation parameters are also incorporated to adapt the thresholding to the severity of multipath propagation. The denoised signal is reconstructed using the inverse Continuous Wavelet Transform, and the performance is evaluated using output Signal-to-Noise Ratio (SNR), Root Mean Square Error (RMSE), Correlation Coefficient (CC), Signal Preservation Index (SPI), computational runtime, and statistical significance analysis. The proposed method is compared with Universal, SURE (Stein's Unbiased Risk Estimate), Minimax, BayesShrink, Empirical Mode Decomposition (EMD)-based, and Variational Mode Decomposition (VMD)-based denoising methods. Monte Carlo simulations show that the proposed hybrid method provides improved denoising performance and better preservation of the transmitted BPSK signal under varying underwater channel conditions.

Keywords: Underwater acoustic communication, binary phase shift keying (BPSK), hybrid adaptive thresholding, multipath propagation, wavelet denoising, ambient noise suppression.

1 Introduction

Underwater acoustic communication has emerged as a key technology for applications such as ocean monitoring, offshore exploration, and autonomous underwater vehicles. Because electromagnetic waves attenuate rapidly in water, acoustic signaling remains the most practical solution for long-range communication. However, underwater acoustic channels are highly challenging because of severe multipath propagation, limited bandwidth, Doppler spread, and high ambient noise. These factors significantly degrade system performance and reliability. Early research on underwater sensor networking has highlighted the fundamental challenges related to varying channel conditions and resource constraints in such environments [1]. In addition, studies on underwater acoustic telemetry have identified limitations in communication performance due to signal distortion and reduced data rates caused by channel characteristics [2]. Propagation-related effects, such as attenuation, delay spread, and channel variability, further underscore the need for robust signal processing techniques in underwater communication systems [3].

To address these challenges, researchers have explored advanced signal processing techniques to improve the reliability of underwater acoustic communication. Wavelet-based signal denoising has emerged as a powerful tool for analyzing non-stationary signals because of its time-frequency localization and multiresolution representation. Traditional wavelet-based denoising approaches often struggle to handle non-stationary and time-varying underwater signals. This motivates more flexible and adaptive methods for suppressing noise while preserving important signal features. Techniques based on tunable wavelet transforms, sparse representations, and adaptive threshold selection have shown improvements in handling non-stationary signals [4,5]. However, most existing methods do not incorporate channel-specific characteristics such as multipath delay spread, which plays a critical role in underwater acoustic communication. Motivated by this limitation, this paper proposes a multipath-aware hybrid wavelet-based denoising framework for underwater acoustic signals. The proposed method integrates Bayesian adaptive thresholding with covariance-assisted coefficient weighting and delay-dependent correlation modeling to adapt the denoising process according to underwater channel conditions.

International Journal of Emerging Research in Engineering, Science, and Management
Vol. 5 | Issue 3 | pp. 81-96 | Jul-Sep 2026.
www.ijeresm.com | eISSN – 2583-4894
Received: 27 Apr 2026 | Revised: 29 Jul 2026 | Accepted: 12 Aug 2026 | Published: 30 Aug 2026

By jointly exploiting signal statistics and channel propagation characteristics, the proposed framework achieves a better balance between effective noise suppression and preserving the transmitted BPSK signal in low-SNR underwater acoustic environments.

2 Literature Review

The communication reliability and system performance of underwater communication systems are inherently challenged by severe multipath propagation, limited bandwidth, and Doppler effects. Earlier foundational research established the relationship between communication capacity and transmission distance in underwater channels and highlighted the impact of attenuation and noise on system performance [6]. Researchers have analyzed acoustic propagation characteristics and channel behavior in underwater environments and emphasized the need for robust signal design and processing techniques for underwater communication systems [7]. Early works on adaptive equalization showed that channel estimation techniques effectively reduce multipath effects and aid signal recovery in underwater environments [8]. Furthermore, dynamic channel conditions and energy constraints were identified as key challenges in underwater acoustic sensor network research, underscoring the importance of efficient communication strategies [9]. To overcome these limitations, chirp-based signaling techniques are used due to their robustness to multipath interference and Doppler shifts.

Chirp-signal-based underwater communication systems provide improved detection performance and low probability of detection/interception capabilities [10]. Advanced modulation schemes such as Orthogonal Chirp Division Multiplexing [11] and multiuser chirp modulation [12] are used to enhance spectral efficiency and for reliable transmission in underwater environments. Recent developments have incorporated multipath-aware communication strategies [13] and generalized chirp-spread-spectrum techniques [14] to enhance resilience to channel distortions and interference. Although these studies primarily focus on communication waveform design, they highlight the importance of addressing channel-induced distortions, which motivates the development of robust denoising techniques for underwater communication signals.

In parallel, signal processing techniques for denoising underwater communication signals were also studied. Wavelet-based methods provide effective analysis in both the time and frequency domains by suppressing noise while preserving important signal features [15]. Classical wavelet thresholding approaches, including soft thresholding [16] and wavelet shrinkage [17], form the foundation of modern denoising techniques. A data-driven threshold selection approach for wavelet-based denoising was proposed for image denoising and compression [18]. Their method adapts the threshold according to the statistical characteristics of the wavelet coefficients rather than relying on a fixed threshold, thereby improving the preservation of important signal components while suppressing noise. However, the method was primarily developed for image denoising and does not explicitly incorporate underwater acoustic channel characteristics such as multipath propagation, delay spread, or channel-dependent coefficient weighting.

Bivariate shrinkage methods exploit inter-scale dependencies among wavelet coefficients to improve denoising performance [19]. Statistical modeling approaches, such as scale mixtures of Gaussians, have also been developed to model dependencies among wavelet coefficients and improve image denoising performance [20]. Wavelet-based denoising with translation-invariant techniques has been developed to improve signal reconstruction and remove unwanted artifacts introduced during denoising [21]. The stationary wavelet transform has been used, along with adaptive shrinkage functions, to improve performance in underwater image processing applications [22]. In addition, hybrid decomposition-based denoising methods have shown improved effectiveness in suppressing non-stationary ambient noise in underwater acoustic environments [23]. An adaptive wavelet denoising method with dynamically adjustable threshold estimation and hardware implementation for real-time high-definition image processing is proposed [24]. Although the method improves threshold adaptability and computational efficiency, it was developed for image processing and does not incorporate underwater acoustic channel characteristics such as multipath delay or channel-aware coefficient weighting.

Table 1. Comparison of the proposed method with representative adaptive wavelet denoising methods.

Work	Adaptive Threshold	Multipath-aware	Covariance Weighting	Delay-dependent Correlation	Real Ambient Noise
Yang *et al.* [25]	✓	✗	✗	✗	✓
Zhang *et al.* [26]	✓	Partial	✗	✗	✓
Xing *et al.* [27]	✓	Partial	✗	✗	✓
Li et al. [28]	✓	✗	✗	✗	✓
Proposed Method	✓	✓	✓	✓	✓

International Journal of Emerging Research in Engineering, Science, and Management
Vol. 5 | Issue 3 | pp. 81-96 | Jul-Sep 2026.
www.ijeresm.com | eISSN – 2583-4894
Received: 27 Apr 2026 | Revised: 29 Jul 2026 | Accepted: 12 Aug 2026 | Published: 30 Aug 2026

Recent studies have further explored hybrid denoising strategies by integrating adaptive wavelet thresholding with advanced signal decomposition techniques. A Tuneable Q-factor Wavelet Transform (TQWT)-based framework was proposed, combining sparse basis pursuit and adaptive wavelet thresholding for underwater acoustic signals. Correlation-based sub-band identification was introduced to improve denoising. Although the proposed method demonstrated robustness to underwater noise, it relied on the signal's statistical characteristics and did not consider underwater channel parameters [25]. An underwater acoustic signal denoising framework based on Ensemble Empirical Mode Decomposition (EEMD), correlation coefficient analysis, permutation entropy, and wavelet threshold denoising was developed. Their hybrid approach effectively improved the output SNR, reduced RMSE, and enhanced the correlation coefficient for both simulated and real underwater acoustic signals.

However, the algorithm does not explicitly incorporate channel-aware adaptive threshold estimation for varying underwater propagation conditions [26]. A denoising method that combines Symplectic Geometry Mode Decomposition (SGMD) with wavelet thresholding was proposed to suppress complex underwater noise. However, the method does not explicitly incorporate channel-aware covariance weighting or delay-dependent threshold adaptation [27]. More recently, a hybrid framework, WDnet, was introduced that combines wavelet denoising with deep learning for enhancing underwater acoustic signals. It significantly improved the denoising performance under complex underwater noise conditions. However, its deep-learning architecture introduces additional training and computational requirements compared with conventional wavelet thresholding methods, which may increase the complexity of real-time implementation [28]. Table 1 summarizes the key characteristics of representative adaptive wavelet denoising methods and compares them with the proposed method.

Despite these advancements, a significant research gap exists. Existing studies address either communication design or wavelet-based denoising independently, without incorporating channel-aware parameters such as multipath delay spread into the denoising process. Based on the studies reviewed in this work, multipath delay spread, delay-dependent correlation, and covariance-assisted coefficient weighting do not appear to have been jointly exploited within a single adaptive wavelet thresholding framework for underwater acoustic signal denoising. To address this gap, the proposed methodology integrates Bayesian adaptive thresholding, covariance-assisted coefficient weighting, and delay-dependent correlation modeling into a unified multipath-aware denoising framework.

3 METHODOLOGY

The proposed methodology consists of signal generation, underwater channel modeling, underwater ambient noise addition, CWT-based time-frequency decomposition, hybrid adaptive wavelet thresholding, signal reconstruction, and performance evaluation. Fig. 1 illustrates the complete framework.

3.1. Signal Generation

A Binary Phase Shift Keying signal is generated to simulate the transmitted underwater acoustic communication signal. The binary data sequence is mapped to bipolar symbols and pulse-shaped with a raised-cosine filter to minimize inter-symbol interference before carrier modulation. The transmitted passband signal is expressed as,

$$s(t) = b(t)\cos(2\pi f_c t) \tag{1}$$

where $b(t)$ denotes the pulse-shaped baseband signal and f_c is the carrier frequency. In this work, the carrier frequency is 10 kHz, the sampling frequency is 32 kHz, and the symbol rate is 1000 symbols/s. The raised cosine filter employs a roll-off factor of 0.25 and a span of six symbols.

3.2. Multipath Channel Modeling

To represent realistic underwater propagation, the transmitted signal is passed through different channel models, including 5-Path, Rayleigh, and Rician fading channels. For the multipath channels, the impulse response is represented as:

$$h(t) = \sum_{i=1}^{L} a_i\, \delta(t - \tau_i) \tag{2}$$

where a_i denotes the gain of the i^{th} propagation path, τ_i represents the corresponding propagation delay, and L is the number of propagation paths. The received multipath signal is

$$x(t) = s(t) * h(t) \tag{3}$$

where * denotes convolution. The simulations consider RMS delay spreads of 2 ms and 3 ms for all multipath channel models investigated in this work.

International Journal of Emerging Research in Engineering, Science, and Management
Vol. 5 | Issue 3 | pp. 81-96 | Jul-Sep 2026.
www.ijeresm.com | eISSN – 2583-4894
Received: 27 Apr 2026 | Revised: 29 Jul 2026 | Accepted: 12 Aug 2026 | Published: 30 Aug 2026

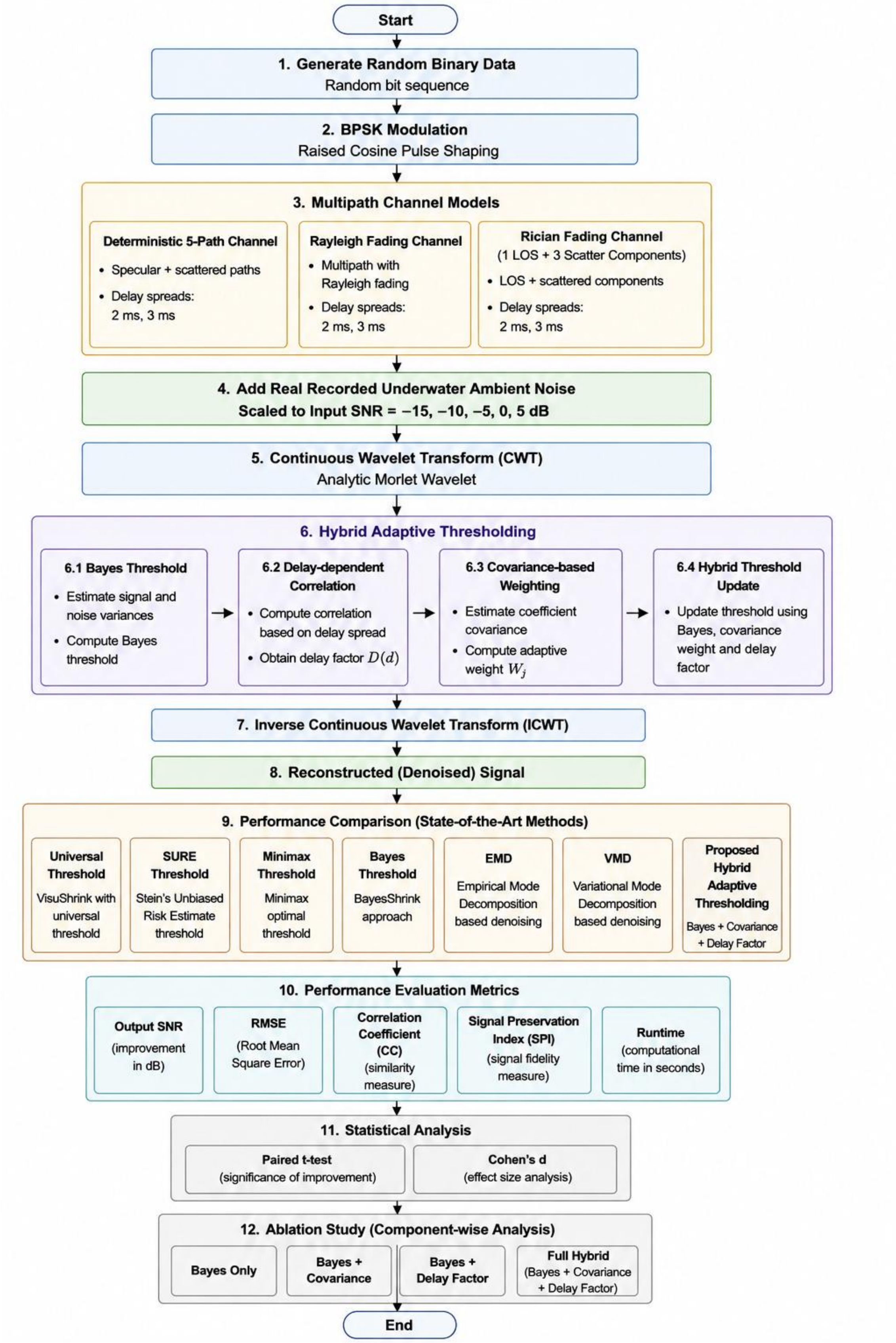

Fig. 1. Overall flow of the proposed hybrid method.

International Journal of Emerging Research in Engineering, Science, and Management
Vol. 5 | Issue 3 | pp. 81-96 | Jul-Sep 2026.
www.ijeresm.com | eISSN – 2583-4894
Received: 27 Apr 2026 | Revised: 29 Jul 2026 | Accepted: 12 Aug 2026 | Published: 30 Aug 2026

For the 5-path channel, the propagation delays are adjusted to achieve the specified RMS delay spread while keeping the path gains fixed. In the Rayleigh channel, each propagation path experiences independent Rayleigh fading with RMS delay spreads of 2 ms and 3 ms. Similarly, the Rician channel consists of four propagation paths: one dominant line-of-sight (LOS) component and three scattered Rayleigh components. The Rician K-factor parameter is set to 5. This enables a consistent evaluation of the proposed denoising algorithm under different multipath propagation conditions. The 5-Path channel represents a separate deterministic multipath model with five propagation paths, whereas the Rayleigh and Rician channels are independent fading channel models. The Rician channel considered in this work consists of one LOS component and three scattered components.

3.3. Noisy signal

The experiments utilized a pinger noise recording obtained from the National Institute of Ocean Technology (NIOT), Chennai, sampled at 25 kHz. The recording consists of 10,500,000 samples, corresponding to a total duration of 420 s. This provides a sufficiently long recording from which different noise segments can be randomly selected for the Monte Carlo simulations. The recorded noise is pre-processed to ensure consistent analysis. It includes removing the DC component to eliminate unwanted low-frequency bias components and amplitude normalization to ensure consistent noise power before scaling and input SNR adjustment. During each Monte Carlo realization, a random segment of the normalized noise having the same length as the transmitted signal was selected and subsequently scaled to the required input SNR level (−15, −10, −5, 0, and 5 dB).

$$scale = \sqrt{\frac{P_{signal}}{P_{noise}10^{SNR/10}}} \tag{4}$$

P_{signal} is the average signal power and P_{noise} is the average noise power. The noisy signal y(t) is given as,

$$y(t) = x(t) + n(t) \tag{5}$$

where n(t) represents the additive underwater ambient noise.

3.4. Time-Frequency Decomposition

The noisy signal is decomposed using the CWT. The wavelet used is the Analytic Morlet [15]. CWT provides a multi-scale representation of the signal and is given by

$$W(s,t) = \int y(\tau)\,\psi^*\left(\frac{\tau - t}{s}\right) d\tau \tag{6}$$

Here $W(s,t)$ represents the wavelet coefficients, $\psi(t)$ is the mother wavelet, $\psi^*(.)$ denotes the complex conjugate of the mother wavelet, s is the scaling parameter, and τ is the translation parameter. Separate wavelet decompositions are computed for both the noisy signal and the noise to support adaptive threshold estimation at each scale.

3.5. Proposed Hybrid Denoising Method

For each CWT scale, the noise variance is first estimated from the CWT coefficients for the noise recording. If $\sigma_n^2(s)$ is the noise variance at scale s,

$$\sigma_n^2(s) = var(W_n(s)) \tag{7}$$

where $W_n(s)$ denotes the CWT coefficients of the noise-only signal at scale s. The variance of the corresponding noisy received signal coefficients is calculated as,

$$\sigma_y^2(s) = var\left(W_y(s)\right) \tag{8}$$

where $W_y(s)$ represents the CWT coefficients of the noisy received signal. Assuming that the observed coefficient variance consists of signal and noise contributions, the signal-related variance $\sigma_x^2(s)$ is estimated by

$$\sigma_x^2(s) = \max\left[\sigma_y^2(s) - \sigma_n^2(s), \epsilon\right] \tag{9}$$

where ϵ is a small positive constant introduced to avoid numerical instability when the estimated signal contribution approaches zero. The corresponding signal standard deviation is obtained as

International Journal of Emerging Research in Engineering, Science, and Management
Vol. 5 | Issue 3 | pp. 81-96 | Jul-Sep 2026.
www.ijeresm.com | eISSN – 2583-4894
Received: 27 Apr 2026 | Revised: 29 Jul 2026 | Accepted: 12 Aug 2026 | Published: 30 Aug 2026

$$\sigma_x(s) = \sqrt{\sigma_x^2(s)} \tag{10}$$

The scale-dependent BayesShrink threshold T [18] is then obtained as

$$T = \frac{\sigma_n^2(s)}{\sigma_x(s)} \tag{11}$$

Thus, the threshold is determined independently at each CWT scale from the estimated noise and signal statistics. A larger noise contribution results in a larger threshold, whereas a stronger estimated signal contribution reduces the threshold, allowing signal-related wavelet coefficients to be retained. The threshold is applied using soft thresholding

$$W_{soft} = sign(W).\max(|W| - T, 0) \tag{12}$$

In soft thresholding (W_{soft}), the coefficients below the threshold are reduced. This helps maintain continuity in the reconstructed signal. Channel-dependent parameters like the correlation factor ρ are incorporated into the adaptive weighting parameter to improve robustness under multipath conditions. The multipath correlation factor is computed as

$$\rho = e^{-\tau_{rms}/\tau_{ref}} \tag{13}$$

The reference delay spread τ_{ref} is set to 0.5 ms. The adaptive weighting parameter γ is calculated as,

$$\gamma = \frac{1}{1 + \tau_{rms}/\tau_{ref}} \tag{14}$$

To incorporate the covariance information into the adaptive weighting, the covariance between adjacent CWT scales is calculated from the noisy received signal coefficients. For two adjacent scales s and s+1, the inter-scale covariance is defined as,

$$C_s = \frac{1}{N-1}\sum_{t=1}^{N}\left(W_y(s,t) - \overline{W_y(s)}\right)\left(W_y(s+1,t) - \overline{W_y(s+1)}\right)^* \tag{15}$$

where $W_y(s,t)$ represent CWT coefficients of the noisy received signal at scale s and time index t, $\overline{W_y(s)}$ represents its mean value at scale s, $(.)^*$ denotes the complex conjugate, and N is the number of CWT time samples. The magnitude of the covariance is normalized using the corresponding scale-dependent coefficient variances to obtain a dimensionless covariance factor,

$$\kappa_s = \frac{|C_s|}{\sqrt{\sigma_y^2(s)\sigma_y^2(s+1) + \epsilon}} \tag{16}$$

The normalized inter-scale covariance factor κ_s quantifies the statistical consistency between adjacent CWT scales. This factor is combined with the delay-dependent correlation factor ρ and weighting parameter γ to obtain the covariance- and delay-assisted weighting factor ω_s. The resulting effective signal variance incorporates both covariance information and the severity of multipath propagation, thereby enabling channel-aware adaptive thresholding.

$$\omega_s = 1 + \gamma\rho\kappa_s \tag{17}$$

The effective signal variance used in the adaptive weighting is consequently expressed as,

$$\sigma_{eff}^2(s) = \sigma_x^2(s)[1 + \gamma\rho\kappa_s] \tag{18}$$

where $\sigma_x^2(s)$ is the estimated signal-related variance obtained from Eq. (9), ρ represents the delay-dependent multipath correlation factor, γ controls the delay-dependent weighting strength, and κ_s represents the normalized inter-scale covariance. Thus, the proposed weighting explicitly incorporates both wavelet-domain covariance information and multipath delay characteristics. The resulting effective variance is therefore a covariance- and delay-adaptive estimate of the signal variance, enabling improved threshold adaptation under time-varying underwater acoustic channels. The adaptive coefficient α is calculated by

$$\alpha(s) = min\left[\frac{\sigma_{eff}^2(s)}{\sigma_{eff}^2(s) + \sigma_n^2(s)}, 0.85\right] \tag{19}$$

International Journal of Emerging Research in Engineering, Science, and Management
Vol. 5 | Issue 3 | pp. 81-96 | Jul-Sep 2026.
www.ijeresm.com | eISSN – 2583-4894
Received: 27 Apr 2026 | Revised: 29 Jul 2026 | Accepted: 12 Aug 2026 | Published: 30 Aug 2026

where α(s) is limited to a maximum value of 0.85 based on empirical evaluation to prevent excessive amplification. The final hybrid denoised coefficients are obtained by combining the original and soft-thresholded coefficients as

$$W_{hybrid}(s,t) = \alpha(s)W_s(s,t) + (1 - \alpha(s))W_{soft} \tag{20}$$

Here $W_s(s,t)$ is the original coefficient and W_{soft} represents the soft-thresholded coefficient. The proposed hybrid method preserves important signal features using the original coefficients and suppresses noise using thresholded coefficients. Unlike conventional methods that rely on thresholded coefficients, the proposed method combines Bayes thresholding with adaptive coefficient weighting to preserve important signal components while suppressing noise. Table 2 summarizes the computational complexity of the denoising methods compared in the paper.

The EMD algorithm performs repeated sifting operations to extract intrinsic mode functions, resulting in a computational complexity of approximately $O(KN^2)$, where K denotes the number of extracted Intrinsic Mode Functions (IMFs), and N is the number of samples. Similarly, VMD requires iterative optimization to estimate multiple signal modes, resulting in a computational complexity of $O(KNI)$, where K denotes the number of modes and I the number of optimization iterations. The proposed hybrid denoising framework requires $O(SN)$ operations, where S is the number of wavelet scales. It includes the Continuous Wavelet Transform and the Inverse Continuous Wavelet Transform. After wavelet decomposition, adaptive threshold estimation, inter-scale covariance estimation, covariance-based weighting, and delay-dependent weighting are calculated for each scale. These operations involve variance and inter-scale covariance estimation together with elementary arithmetic operations and therefore do not increase the asymptotic computational complexity.

Table 2. Computational complexity of the compared denoising methods.

Method	Dominant Operations	Computational Complexity
Universal Threshold	CWT + thresholding + ICWT	$O(SN)$
SURE Threshold	CWT + adaptive threshold selection + ICWT	$O(SN)$
Minimax Threshold	CWT + threshold computation + ICWT	$O(SN)$
Bayes Threshold	CWT + variance estimation + ICWT	$O(SN)$
Proposed Hybrid	CWT + covariance estimation + delay weighting + adaptive thresholding + ICWT	$O(SN)$
EMD	Iterative empirical mode decomposition	$O(KN^2)$
VMD	Iterative variational optimization	$O(KNI)$

Therefore, the overall asymptotic computational complexity of the proposed algorithm remains of the same order as that of conventional CWT-based thresholding approaches such as Universal, SURE, Minimax, and Bayes thresholding. Thus, the proposed approach maintains the same asymptotic computational complexity, O(SN), as conventional CWT-based thresholding methods while incorporating additional adaptive weighting operations. To evaluate the contribution of each component of the proposed hybrid framework, an ablation study is performed.

Four configurations are investigated:

i. Bayes thresholding alone,
ii. Bayes thresholding with covariance-based weighting,
iii. Bayes thresholding with delay-adaptive weighting, and
iv. the complete hybrid method combining both covariance weighting and delay-dependent adaptation.

Section 4 presents and discusses the corresponding results.

3.6. Signal Reconstruction

The signal is reconstructed using the Inverse Continuous Wavelet Transform (ICWT).

$$\hat{x}(t) = ICWT(W_{hybrid}) \tag{21}$$

For comparison, Universal, SURE, Minimax, Bayes, Empirical Mode Decomposition, and Variational Mode Decomposition are also implemented.

International Journal of Emerging Research in Engineering, Science, and Management
Vol. 5 | Issue 3 | pp. 81-96 | Jul-Sep 2026.
www.ijeresm.com | eISSN – 2583-4894
Received: 27 Apr 2026 | Revised: 29 Jul 2026 | Accepted: 12 Aug 2026 | Published: 30 Aug 2026

3.7. Performance Evaluation

The denoising performance is evaluated using Output SNR, RMSE, Correlation coefficient, Signal preservation index, computational runtime, Monte Carlo simulations, and statistical significance analysis.

Output SNR: Reconstruction quality is measured using output SNR, as given in Eq. (22).

$$SNR_{out} = 10 * \log_{10}\left(\frac{P_{signal}}{P_{error}}\right) \tag{22}$$

Here, error power is given by

$$P_{error} = \frac{1}{N}\|x(t) - \hat{x}(t)\|^2 \tag{23}$$

where $x(t)$ represents the clean received signal, $\hat{x}(t)$ is the reconstructed signal, and N is the number of samples.

Root Mean Square Error: The reconstruction error is quantified using RMSE, as given in Eq. (24).

$$RMSE = \sqrt{\frac{1}{N}\sum_{i=1}^{N}(x_i - \hat{x}_i)^2} \tag{24}$$

where $x_i$and $\hat{x}_i$ denote the clean and reconstructed signals, respectively. Lower RMSE values indicate better reconstruction accuracy.

Correlation Coefficient: The correlation coefficient evaluates the similarity between the clean and reconstructed signals.

$$CC = \frac{\sum(x_i - \bar{x})(\hat{x}_i - \bar{\hat{x}})}{\sqrt{\sum(x_i - \bar{x})^2 \sum(\hat{x}_i - \bar{\hat{x}})^2}} \tag{25}$$

A CC value closer to 1 indicates higher similarity.

Signal Preservation Index: The SPI quantifies how effectively the original signal characteristics are preserved.

$$SPI = 1 - \frac{\| x - \hat{x} \|^2}{\| x \|^2} \tag{26}$$

Higher SPI values indicate better preservation of the original signal characteristics.

Runtime: The computational complexity of each denoising algorithm is assessed by measuring the average execution time over 200 Monte Carlo trials. Runtime indicates the algorithm's computational efficiency and suitability for practical implementation.

Monte Carlo Simulation: For every combination of input SNR, channel model, and delay spread, 200 independent Monte Carlo simulations are performed. During each realization, a new random BPSK bit sequence is generated, a different random segment is selected from the recorded underwater noise, and independent fading coefficients are generated for the Rayleigh and Rician channel models. This produces statistically independent realizations while preserving the channel characteristics and target input SNR.

Statistical Validation: Statistical significance is assessed using paired *t*-tests by comparing the proposed hybrid algorithm with Bayes, EMD, and VMD. Statistical significance is determined using a significance level of $\alpha = 0.05$. In addition to the p-value, Cohen's d effect size is reported to assess both the statistical and practical significance of the observed improvements.

4 Results and Discussion

The proposed hybrid adaptive wavelet thresholding method was evaluated using 200 Monte Carlo simulations to ensure statistical stability. A BPSK signal with a carrier frequency of 10 kHz was generated at a sampling frequency of 32 kHz and a symbol rate of 1000 symbols/s. The recorded noise was resampled from 25 kHz to the 32 kHz sampling frequency of the communication signal before noise addition. Pulse shaping was carried out using a raised-cosine filter with a roll-off factor of 0.25 and a span of 6 symbols. Real underwater ambient noise dominated by pinger noise was added to the BPSK signal.

The received signal was scaled to input SNRs of -15 dB, -10 dB, -5 dB, 0 dB, and 5 dB and then transmitted through a 5-path, Rayleigh, and Rician underwater acoustic channel model with multipath delays of 2 and 3 ms. The Rayleigh fading channel was modeled using three independently faded multipath components with path gains of 1, 0.6, and 0.4. All simulations were performed in MATLAB R2022a on a Windows 11 (64-bit) workstation equipped with an Intel Core Ultra 5 processor and 16 GB RAM. The reported runtimes correspond to the average execution time obtained over 200 independent Monte Carlo realizations. The denoising performance was compared with Bayes, Universal, SURE (Stein's Unbiased Risk Estimate), Minimax, EMD (Empirical Mode Decomposition), and VMD (Variational Mode Decomposition) methods. The performance was evaluated using output SNR, RMSE, correlation coefficient, SPI, and computational runtime. Statistical significance was evaluated using a paired *t*-test at $\alpha = 0.05$, and the practical significance of the observed differences was quantified using Cohen's *d*.

Table 3 presents the output SNR for the 5-path channel under different input SNRs and delay spreads. Fig. 2 show the time-frequency representations of the noisy and hybrid-denoised BPSK signals corresponding to the highest output SNR obtained during the 200 Monte Carlo simulations for the 5-Path model at an input SNR of 5 dB and an RMS delay spread of 3 ms.

Table 3. Output SNR (dB) for the 5-Path channel under different input SNRs and delay spreads.

Input SNR (dB)	Delay (ms)	EMD	VMD	Universal	SURE	Minimax	Bayes	Hybrid
-15	2	-15.010	-13.064	-8.895	-7.229	-4.824	-0.691	-0.261
-15	3	-15.003	-13.116	-9.251	-7.740	-5.381	-0.644	-0.236
-10	2	-9.996	-8.134	-5.203	-3.953	-3.216	0.736	1.698
-10	3	-10.014	-8.072	-5.106	-3.635	-2.996	0.395	1.342
-5	2	-5.000	-2.840	-0.885	-0.211	-1.151	3.131	4.169
-5	3	-5.014	-2.913	-1.069	-0.672	-1.477	3.392	4.424
0	2	-0.019	3.334	2.532	2.182	-0.339	6.552	7.455
0	3	-0.022	2.679	2.650	2.263	-0.148	6.656	7.529
5	2	5.024	9.795	6.393	4.771	0.649	9.691	10.382
5	3	5.064	9.711	6.422	4.710	0.664	9.744	10.438

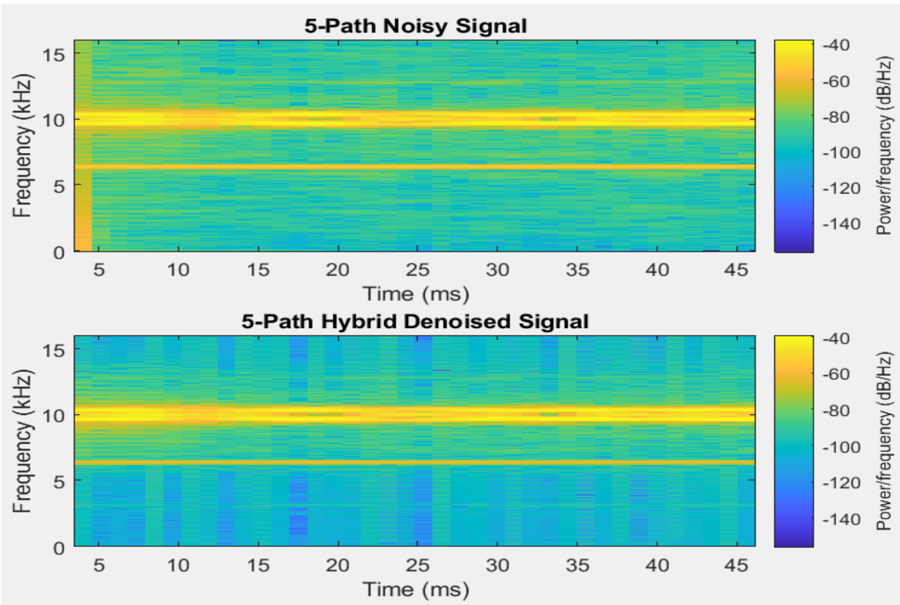

Fig. 2. Time-frequency representation of the 5-Path channel signal corresponding to the highest output SNR before and after the proposed hybrid adaptive wavelet denoising (input SNR = 5 dB, RMS delay spread = 3 ms).

The proposed method achieves a higher output SNR than the conventional denoising methods across the investigated 5-Path conditions, with particularly clear improvements at low input SNRs. Fig. 2 further illustrates the preservation of the dominant signal components after denoising. The robustness of the proposed method under Rayleigh and Rician fading channels is subsequently evaluated using Tables 4 and 5 and Figs. 3 and 4.

International Journal of Emerging Research in Engineering, Science, and Management
Vol. 5 | Issue 3 | pp. 81-96 | Jul-Sep 2026.
www.ijeresm.com | eISSN – 2583-4894
Received: 27 Apr 2026 | Revised: 29 Jul 2026 | Accepted: 12 Aug 2026 | Published: 30 Aug 2026

Table 4. Output SNR (dB) for the Rayleigh channel under different input SNRs and delay spreads.

Input SNR (dB)	Delay (ms)	EMD	VMD	Universal	SURE	Minimax	Bayes	Proposed
-15	2	-15.021	-13.271	-10.130	-8.639	-6.457	-0.832	-0.414
-15	3	-15.039	-13.234	-10.061	-8.453	-6.390	-0.862	-0.446
-10	2	-10.043	-8.222	-5.286	-3.803	-3.173	0.718	1.715
-10	3	-10.039	-8.213	-5.586	-4.076	-3.583	0.676	1.658
-5	2	-5.022	-2.945	-1.158	-0.734	-1.535	3.117	4.222
-5	3	-5.019	-2.863	-1.027	-0.634	-1.535	3.254	4.351
0	2	-0.046	3.008	2.833	2.013	-0.284	6.367	7.297
0	3	-0.056	2.989	2.699	1.855	-0.363	6.549	7.457
5	2	5.055	9.922	6.505	3.744	0.380	9.446	10.193
5	3	5.045	9.873	6.483	3.937	0.369	9.584	10.324

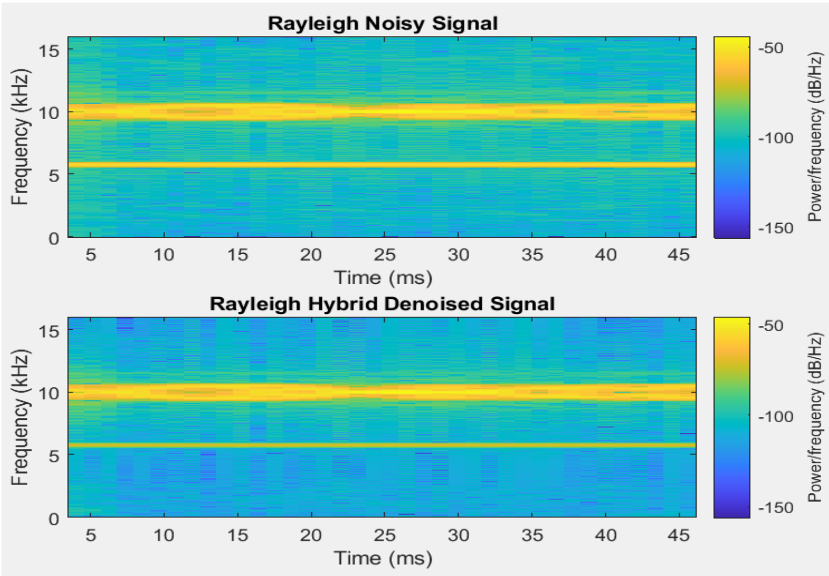

Fig. 3. Time-frequency representation of the Rayleigh channel signal corresponding to the highest output SNR before and after the proposed hybrid adaptive wavelet denoising (input SNR = 5 dB, RMS delay spread = 3 ms).

Table 5. Output SNR (dB) for the Rician channel under different input SNRs and delay spreads.

Input SNR (dB)	Delay (ms)	EMD	VMD	Universal	SURE	Minimax	Bayes	Hybrid
-15	2	-15.030	-13.099	-9.118	-7.522	-4.924	-0.534	-0.167
-15	3	-15.025	-13.136	-9.512	-7.923	-5.533	-0.391	0.072
-10	2	-10.013	-8.138	-5.204	-4.155	-3.106	0.561	1.579
-10	3	-10.008	-8.060	-4.871	-3.875	-3.029	0.312	1.330
-5	2	-4.989	-2.968	-1.364	-1.830	-2.038	2.986	4.241
-5	3	-5.025	-2.764	-0.935	-1.242	-1.538	2.834	4.007
0	2	-0.015	2.970	2.753	0.116	-0.649	6.354	7.382
0	3	-0.074	2.848	2.824	0.645	-0.553	6.255	7.262
5	2	5.021	9.635	6.309	0.864	-0.182	9.486	10.316
5	3	5.018	9.868	6.554	1.794	0.013	9.336	10.169

Figs. 3 and 4 further illustrate the preservation of the dominant signal components after hybrid denoising under the Rayleigh and Rician channel conditions, respectively. Tables 3–5 compare the output SNR achieved by the proposed hybrid wavelet thresholding method with the Universal, SURE, Minimax, Bayes, EMD, and VMD algorithms under 5-Path, Rayleigh, and Rician channel conditions for different input SNRs and delay spreads. The proposed hybrid method achieves the highest output SNR across all investigated scenarios. It demonstrates its superior denoising capability under both severe and moderate noise conditions. At low input SNRs such as -15 dB and -10 dB, conventional thresholding methods struggle to distinguish signal components from underwater noise. The proposed hybrid approach incorporates multipath-aware adaptive weighting based on channel characteristics. EMD performance is comparatively low for all SNR conditions considered. VMD performance improves with higher SNR, but remains limited compared to the proposed hybrid method. Beyond output SNR, reconstruction accuracy and signal preservation were further assessed using RMSE, correlation coefficient, and SPI, as summarized in Table 6.

International Journal of Emerging Research in Engineering, Science, and Management
Vol. 5 | Issue 3 | pp. 81-96 | Jul-Sep 2026.
www.ijeresm.com | eISSN – 2583-4894
Received: 27 Apr 2026 | Revised: 29 Jul 2026 | Accepted: 12 Aug 2026 | Published: 30 Aug 2026

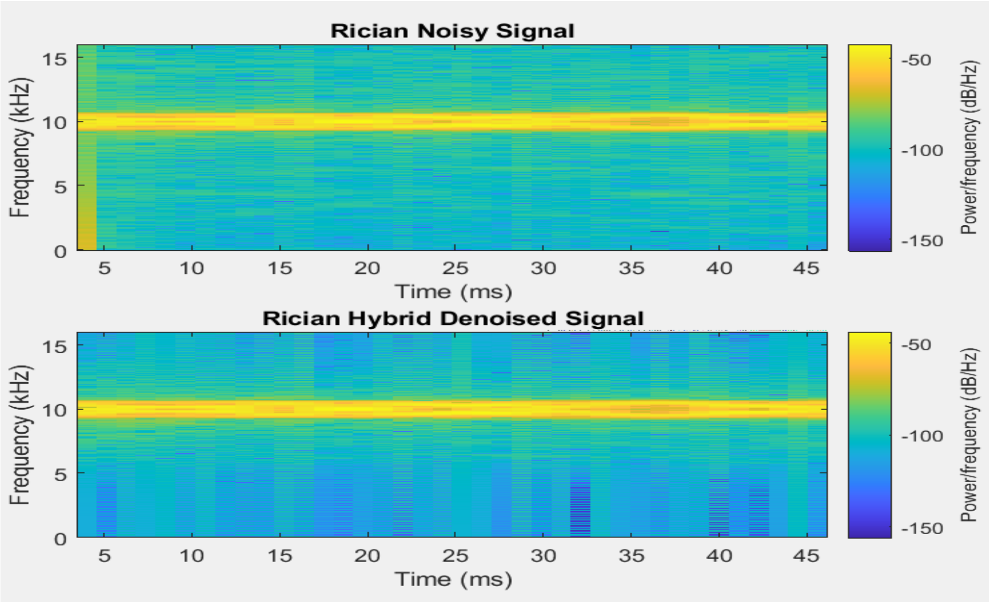

Fig. 4. Time-frequency representation of the Rician channel signal corresponding to the highest output SNR before and after the proposed hybrid adaptive wavelet denoising (input SNR = 5 dB, RMS delay spread = 2 ms).

Table 6. Comparison of RMSE, correlation coefficient, and signal preservation index between the Bayes and proposed hybrid methods.

Channel	Input SNR (dB)	Delay (ms)	RMSE		Correlation coefficient		Signal Preservation Index	
			Bayes	Proposed	Bayes	Proposed	Bayes	Proposed
5-Path	-15	2	0.19175	0.17456	0.32346	0.53152	-0.00383	0.21432
		3	0.21637	0.19641	0.34145	0.54089	0.01125	0.22403
	-10	2	0.16029	0.14304	0.36542	0.55028	0.05262	0.24917
		3	0.18143	0.16227	0.33451	0.52855	0.01562	0.21602
	-5	2	0.12225	0.10771	0.71085	0.77096	0.47709	0.59419
		3	0.12812	0.11390	0.73600	0.78191	0.50679	0.61139
	0	2	0.08165	0.07399	0.89857	0.90122	0.76376	0.80537
		3	0.08983	0.08135	0.89992	0.90253	0.76490	0.80680
	5	2	0.05684	0.05239	0.96347	0.96150	0.88576	0.90310
		3	0.06381	0.05877	0.96270	0.96070	0.88372	0.90144
Rayleigh	-15	2	0.15838	0.15167	0.14000	0.33976	-0.35246	-0.25000
		3	0.17349	0.16603	0.15453	0.35190	-0.33107	-0.23393
	-10	2	0.13949	0.12378	0.33455	0.54103	0.02371	0.23557
		3	0.14148	0.12601	0.34278	0.53856	0.02979	0.23302
	-5	2	0.10004	0.08769	0.69742	0.76268	0.45641	0.58274
		3	0.10544	0.09291	0.72160	0.77588	0.48821	0.60242
	0	2	0.06734	0.06036	0.89804	0.90308	0.76150	0.80771
		3	0.07012	0.06301	0.89891	0.90280	0.76218	0.80712
	5	2	0.04621	0.04229	0.96187	0.96032	0.88212	0.90126
		3	0.05037	0.04612	0.96334	0.96202	0.88567	0.90409
Rician	-15	2	0.13487	0.12692	0.15453	0.35190	-0.35073	-0.25231
		3	0.14853	0.14037	0.13689	0.34576	-0.33107	-0.23393
	-10	2	0.11386	0.10087	0.30561	0.52764	-0.00198	0.21774
		3	0.11989	0.10635	0.30028	0.51576	-0.02422	0.19675
	-5	2	0.08515	0.07351	0.69132	0.77043	0.45470	0.59387
		3	0.09020	0.07869	0.68160	0.75671	0.43913	0.57344
	0	2	0.05725	0.05081	0.89081	0.89970	0.74889	0.80221
		3	0.06057	0.05393	0.88993	0.89788	0.74660	0.79909
	5	2	0.03965	0.03597	0.96215	0.96164	0.88237	0.90345
		3	0.04173	0.03786	0.96029	0.95957	0.87840	0.90020

International Journal of Emerging Research in Engineering, Science, and Management
Vol. 5 | Issue 3 | pp. 81-96 | Jul-Sep 2026.
www.ijeresm.com | eISSN – 2583-4894
Received: 27 Apr 2026 | Revised: 29 Jul 2026 | Accepted: 12 Aug 2026 | Published: 30 Aug 2026

Among the conventional approaches, the Bayes method performs better because of its adaptive statistical threshold estimation. However, the proposed hybrid method consistently improves SNR over Bayes across all investigated channel models. The improvements also remained stable for different delay spreads (2 ms and 3 ms). This indicates that the proposed algorithm is robust to variations in multipath propagation and channel dynamics. Table 6 presents RMSE, correlation coefficient, and signal preservation index values of the Bayes and proposed hybrid methods under different channel conditions and delay spreads. The proposed hybrid method consistently achieves a lower RMSE than the conventional Bayes thresholding across the 5-path, Rayleigh, and Rician channels. The reduced reconstruction error indicates that the hybrid method's adaptive, multipath-aware weighting preserves the original signal more accurately, especially in low-SNR environments.

The proposed hybrid achieves a higher correlation than Bayes under most channel conditions. This indicates improved waveform preservation after denoising. Although Bayes exhibits a marginally higher correlation at 5 dB in a few cases, the hybrid consistently maintains strong signal similarity. These results indicate that the proposed adaptive threshold provides a favorable balance between denoising performance and signal fidelity. The hybrid method achieves higher SPI values than Bayes across all channels and input SNR levels investigated. This indicates improved preservation of the transmitted acoustic signal while minimizing distortion. The improvement is greater under severe noise conditions. This demonstrates the robustness of the proposed thresholding strategy.

Table 7. Average runtime comparison.

Algorithm	Average Runtime (s)
Bayes	0.010324
Hybrid	0.023660
EMD	0.053552
VMD	0.066111

Table 7 summarizes the average computational runtime of each denoising algorithm. The proposed hybrid method requires more computational time than conventional Bayes thresholding because of the additional adaptive weighting and multipath parameter estimation. However, its runtime remains lower than that of VMD and EMD while providing improved denoising performance. This trade-off demonstrates that the proposed hybrid algorithm offers an effective balance between computational complexity and reconstruction quality, making it suitable for practical underwater acoustic communication systems.

Table 8. Ablation study of the proposed hybrid method under the 5-path channel.

Input SNR (dB)	Bayes Only	Bayes + Covariance	Bayes + Delay Factor	Full Hybrid
-15	-0.0199	0.2086	0.2196	0.2205
-10	0.7900	1.7010	1.7405	1.7435
-5	3.2398	4.2923	4.3084	4.3093
0	6.5250	7.3769	7.3778	7.3776
5	9.6260	10.3180	10.3200	10.3200

Table 9. Ablation study of the proposed hybrid method under a Rayleigh channel.

Input SNR (dB)	Bayes Only	Bayes + Covariance	Bayes + Delay Factor	Full Hybrid
-15	-0.8324	-0.4568	-0.4173	-0.4136
-10	0.6563	1.6033	1.6483	1.6518
-5	2.9393	4.0490	4.0697	4.0710
0	6.5829	7.5043	7.5096	7.5098
5	9.4508	10.2030	10.2060	10.2070

Table 10. Ablation study of the proposed hybrid method under a Rician channel.

Input SNR (dB)	Bayes Only	Bayes + Covariance	Bayes + Delay Factor	Full Hybrid
-15	-0.5881	-0.1621	-0.1415	-0.1400
-10	0.5612	1.5282	1.5754	1.5791
-5	2.9855	4.2073	4.2386	4.2410
0	6.3542	7.3721	7.3813	7.3818
5	9.4862	10.3100	10.3150	10.3160

The ablation results in Tables 8 to 10 show the individual contributions of covariance-based weighting and the multipath delay factor under the investigated channel conditions.

International Journal of Emerging Research in Engineering, Science, and Management
Vol. 5 | Issue 3 | pp. 81-96 | Jul-Sep 2026.
www.ijeresm.com | eISSN – 2583-4894
Received: 27 Apr 2026 | Revised: 29 Jul 2026 | Accepted: 12 Aug 2026 | Published: 30 Aug 2026

Compared with the Bayes-only baseline, incorporating covariance-based adaptive weighting improves the output SNR by enhancing the discrimination between signal- and noise-dominated coefficients. Adding the delay-dependent factor further improves performance by adapting the threshold to the severity of multipath propagation. Combining both components in the full hybrid configuration generally produces the highest output SNR. These results indicate that the covariance and delay-aware components contribute complementary information to the proposed denoising framework. Table 11 presents a statistical comparison of the proposed hybrid denoising method with the Bayes, EMD, and VMD algorithms for a 3 ms multipath delay spread across the 5-Path, Rayleigh, and Rician channel models, with varying input SNR.

Table 11. Statistical comparison of the proposed hybrid method with Bayes, EMD, and VMD for a 3 ms delay spread.

Channel	Input SNR (dB)	Comparison	p-value	Cohen's d	Interpretation
5-Path	**-15**	Proposed vs Bayes	< 0.001	2.06	Significant
		Proposed vs EMD	< 0.001	5.37	Significant
		Proposed vs VMD	< 0.001	4.44	Significant
	-10	Proposed vs Bayes	< 0.001	3.96	Significant
		Proposed vs EMD	< 0.001	4.73	Significant
		Proposed vs VMD	< 0.001	3.24	Significant
	-5	Proposed vs Bayes	< 0.001	3.09	Significant
		Proposed vs EMD	< 0.001	5.02	Significant
		Proposed vs VMD	< 0.001	2.72	Significant
	0	Proposed vs Bayes	< 0.001	3.73	Significant
		Proposed vs EMD	< 0.001	4.63	Significant
		Proposed vs VMD	< 0.001	1.27	Significant
	5	Proposed vs Bayes	< 0.001	4.96	Significant
		Proposed vs EMD	< 0.001	4.39	Significant
		Proposed vs VMD	0.037	0.15	Significant
Rayleigh	**-15**	Proposed vs Bayes	< 0.001	1.70	Significant
		Proposed vs EMD	< 0.001	4.88	Significant
		Proposed vs VMD	< 0.001	4.10	Significant
	-10	Proposed vs Bayes	< 0.001	3.99	Significant
		Proposed vs EMD	< 0.001	4.72	Significant
		Proposed vs VMD	< 0.001	3.21	Significant
	-5	Proposed vs Bayes	< 0.001	3.21	Significant
		Proposed vs EMD	< 0.001	4.54	Significant
		Proposed vs VMD	< 0.001	2.56	Significant
	0	Proposed vs Bayes	< 0.001	3.95	Significant
		Proposed vs EMD	< 0.001	4.33	Significant
		Proposed vs VMD	< 0.001	1.54	Significant
	5	Proposed vs Bayes	< 0.001	5.23	Significant
		Proposed vs EMD	< 0.001	4.98	Significant
		Proposed vs VMD	0.267	0.08	Not Significant
Rician	**-15**	Proposed vs Bayes	< 0.001	1.79	Significant
		Proposed vs EMD	< 0.001	5.79	Significant
		Proposed vs VMD	< 0.001	4.89	Significant
	-10	Proposed vs Bayes	< 0.001	3.86	Significant
		Proposed vs EMD	< 0.001	4.70	Significant
		Proposed vs VMD	< 0.001	3.33	Significant
	-5	Proposed vs Bayes	< 0.001	3.52	Significant
		Proposed vs EMD	< 0.001	4.80	Significant
		Proposed vs VMD	< 0.001	2.73	Significant
	0	Proposed vs Bayes	< 0.001	4.58	Significant
		Proposed vs EMD	< 0.001	4.50	Significant
		Proposed vs VMD	< 0.001	1.51	Significant
	5	Proposed vs Bayes	< 0.001	6.32	Significant
		Proposed vs EMD	< 0.001	4.79	Significant
		Proposed vs VMD	0.133	0.11	Not Significant

The hybrid algorithm achieves higher output SNR than VMD under low and moderate SNR conditions (-15 dB, -10 dB, -5 dB, and 0 dB) across all channel models. At 5 dB, the difference remains statistically significant for the 5-Path channel (p = 0.037), whereas it is not statistically significant for the Rayleigh (p = 0.267) and Rician (p = 0.133) channels. This behavior may be attributed to the reduced impact of noise at higher SNRs, resulting in more similar reconstruction performance between the methods. Compared with VMD, statistically significant differences are observed mainly under low and moderate SNR conditions; at 5 dB, the difference is significant for the 5-Path channel but not for the Rayleigh and Rician channels. Overall, the experimental results, ablation studies, and statistical analyses consistently confirm that the proposed hybrid algorithm provides reliable, robust, and computationally efficient denoising for underwater acoustic communication systems.

5 CONCLUSION

This paper presented a multipath-aware hybrid adaptive wavelet thresholding algorithm for denoising underwater acoustic communication signals under realistic multipath propagation and ambient underwater noise conditions. The proposed method combines covariance-based adaptive weighting with multipath-delay-aware threshold adaptation to improve noise suppression and preserve useful signal components. The algorithm was evaluated using 200 Monte Carlo simulations under the 5-Path, Rayleigh, and Rician underwater acoustic channel models, with input SNRs ranging from -15 dB to 5 dB and RMS delay spreads of 2 and 3 ms. Experimental results showed that the proposed hybrid algorithm achieved higher output SNR, lower RMSE, improved waveform correlation, and a higher Signal Preservation Index than the conventional Universal, SURE, Bayes, Minimax, EMD, and VMD methods. The improvements were particularly noticeable under severe noise conditions where the proposed method effectively distinguished noise and signal components. The ablation study showed that both covariance-based adaptive weighting and multipath delay compensation improve denoising performance, with the full hybrid configuration generally achieving the highest output SNR across the investigated channel models. The consistent performance gains across the three channel models indicate that incorporating both signal-domain statistics and channel-dependent characteristics enhances the robustness of the denoising framework under varying underwater propagation conditions.

The proposed method requires slightly higher computational time than conventional Bayes thresholding because of the additional covariance and delay-dependent weighting operations. However, its runtime remains lower than those of EMD and VMD. Statistical validation using paired t-tests and Cohen's d demonstrated statistically significant improvements over Bayes and EMD across all investigated SNR conditions. At 5 dB input SNR, the improvement over VMD was statistically significant for the 5-Path channel (p = 0.037), whereas the differences were not statistically significant for the Rayleigh (p = 0.267) and Rician (p = 0.133) channels. Overall, the proposed framework provides an effective balance between denoising accuracy, signal preservation, robustness to multipath propagation, and computational efficiency. This makes it a promising solution for reliable underwater acoustic communication systems in noise-dominated environments. Future work will focus on extending the proposed framework to real-time underwater communication systems, adaptive modulation scenarios, Doppler-affected channels, and experimental validation using sea-trial measurements. Further investigation will consider computational optimization and validation with diverse real-world underwater noise conditions to assess the generalizability of the proposed approach.

FUNDING INFORMATION

This work was supported by the Ministry of Earth Sciences (MoES), Government of India, under the Deep Ocean Mission project (F.No. MoES/PAMC/DOM/165/2023; E-14641).

ACKNOWLEDGMENT

The authors express their sincere gratitude to the National Institute of Ocean Technology (NIOT), Chennai, for providing the necessary research facilities, infrastructure, and technical support that enabled the successful completion of this work.

ETHICS STATEMENT

This study did not involve human or animal subjects and, therefore, did not require ethical approval.

STATEMENT OF CONFLICT OF INTERESTS

The authors declare no conflicts of interest related to this study.

REFERENCES

[1] J. Heidemann, W. Ye, J. Wills, A. Syed, and Y. Li, "Research challenges and applications for underwater sensor networking," *IEEE Wireless Communications and Networking Conference, 2006. WCNC 2006.*, Las Vegas, NV, 2006, pp. 228-235, doi: 10.1109/WCNC.2006.1683469.

[2] D. B. Kilfoyle and A. B. Baggeroer, "The state of the art in underwater acoustic telemetry," *IEEE Journal of Oceanic Engineering*, vol. 25, no. 1, pp. 4-27, Jan. 2000, doi: 10.1109/48.820733.

[3] J. Preisig, "Acoustic propagation considerations for underwater acoustic communications network development," *ACM SIGMOBILE Mobile Computing and Communications Review*, vol. 11, no. 4, pp. 2–10, Oct. 2007, doi: 10.1145/1347364.1347370.

[4] I. W. Selesnick, "Wavelet Transform with Tunable Q-Factor," *IEEE Transactions on Signal Processing*, vol. 59, no. 8, pp. 3560-3575, Aug. 2011, doi: 10.1109/TSP.2011.2143711.

[5] J.-L. Starck, F. Murtagh and J. Fadili, *Sparse Image and Signal Processing: Wavelets, Curvelets, Morphological Diversity*, Cambridge University Press, 2015, doi: 10.1017/CBO9781316104514.

[6] M. Stojanovic, "On the relationship between capacity and distance in an underwater acoustic communication channel," *ACM SIGMOBILE Mobile Computing and Communications Review*, vol. 11, no. 4, pp. 34–43, Oct. 2007, doi: 10.1145/1347364.1347373.

[7] M. Stojanovic, "Recent advances in high-speed underwater acoustic communications," *IEEE Journal of Oceanic Engineering*, vol. 21, no. 2, pp. 125-136, April 1996, doi: 10.1109/48.486787.

[8] M. Stojanovic, L. Freitag and M. Johnson, "Channel-estimation-based adaptive equalization of underwater acoustic signals," *Oceans '99. MTS/IEEE. Riding the Crest into the 21st Century. Conference and Exhibition. Conference Proceedings (IEEE Cat. No.99CH37008)*, Seattle, WA, USA, 1999, pp. 985-990, vol. 2, doi: 10.1109/OCEANS.1999.805007.

[9] I. F. Akyildiz, D. Pompili, and T. Melodia, "Underwater acoustic sensor networks: research challenges," *Ad Hoc Networks*, vol. 3, no. 3, pp. 257–279, Feb. 2005, doi: 10.1016/j.adhoc.2005.01.004.

[10] E. Demirors and T. Melodia, "Chirp-Based LPD/LPI Underwater Acoustic Communications with Code-Time-Frequency Multidimensional Spreading," *Proceedings of the 11th International Conference on Underwater Networks & Systems*, Oct. 2016, doi: 10.1145/2999504.3001083.

[11] Y. Bai and P.-J. Bouvet, "Orthogonal chirp Division multiplexing for underwater acoustic communication," *Sensors*, vol. 18, no. 11, p. 3815, Nov. 2018, doi: 10.3390/s18113815.

[12] F. Yuan, Q. Wei, and E. Cheng, "Multiuser chirp modulation for underwater acoustic channel based on VTRM," *International Journal of Naval Architecture and Ocean Engineering*, vol. 9, no. 3, pp. 256–265, Oct. 2016, doi: 10.1016/j.ijnaoe.2016.09.004.

[13] W. Xie, E. Zhang, L. You, D. Wang, Z. Wang and F. Liqun, "Combating Multi-Path Interference to Improve Chirp-Based Underwater Acoustic Communication," *ICC 2024 - IEEE International Conference on Communications*, Denver, CO, USA, 2024, pp. 5377-5382, doi: 10.1109/ICC51166.2024.10623112.

[14] J. Kim, S. Han, B. Seo, Y. Kim, and H. Lee, "Generalized CHIRP spread spectrum for underwater acoustic communications," *Electronics*, vol. 14, no. 5, p. 964, Feb. 2025, doi: 10.3390/electronics14050964.

[15] S. Mallat, *A wavelet tour of signal processing: The sparse way*. Academic Press, 2015. doi: 10.1016/B978-0-12-374370-1.X0001-8.

[16] D. L. Donoho, "De-noising by soft-thresholding," *IEEE Transactions on Information Theory*, vol. 41, no. 3, pp. 613-627, May 1995, doi: 10.1109/18.382009.

[17] D. L. Donoho and I. M. Johnstone, "Adapting to Unknown Smoothness via Wavelet Shrinkage," *Journal of the American Statistical Association*, vol. 90, no. 432, pp. 1200-1224, 1995, doi: 10.1080/01621459.1995.10476626.

[18] S. G. Chang, B. Yu and M. Vetterli, "Adaptive wavelet thresholding for image denoising and compression," *IEEE Transactions on Image Processing*, vol. 9, no. 9, pp. 1532-1546, Sept. 2000, doi: 10.1109/83.862633.

[19] L. Sendur and I. W. Selesnick, "Bivariate shrinkage functions for wavelet-based denoising exploiting interscale dependency," *IEEE Transactions on Signal Processing*, vol. 50, no. 11, pp. 2744-2756, Nov. 2002, doi: 10.1109/TSP.2002.804091.

[20] J. Portilla, V. Strela, M. J. Wainwright and E. P. Simoncelli, "Image denoising using scale mixtures of Gaussians in the wavelet domain," *IEEE Transactions on Image Processing*, vol. 12, no. 11, pp. 1338-1351, Nov. 2003, doi: 10.1109/TIP.2003.818640.

[21] R. R. Coifman and D. L. Donoho, "Translation-Invariant De-Noising," in *Lecture notes in statistics*, 1995, pp. 125–150. doi: 10.1007/978-1-4612-2544-7_9.

[22] P. Ravisankar, "Underwater acoustic image denoising using stationary wavelet transform and various shrinkage functions," *ELCVIA Electronic Letters on Computer Vision and Image Analysis*, vol. 20, no. 2, Sep. 2021, doi: 10.5565/rev/elcvia.1360.

[23] H. Yang, M. Lai, and G. Li, "Novel underwater acoustic signal denoising: Combined optimization secondary decomposition coupled with original component processing algorithms," *Chaos Solitons & Fractals*, vol. 193, p. 116098, Feb. 2025, doi: 10.1016/j.chaos.2025.116098.

[24] X. Wang and J. Zhao, "Adaptive threshold Wavelet denoising method and hardware implementation for HD Real-Time processing," *Electronics*, vol. 14, no. 11, p. 2130, May 2025, doi: 10.3390/electronics14112130.

[25] J. Yang, S. Yan, L. Mao, Z. Sui, W. Wang, and D. Zeng, "Underwater acoustic signal denoising based on sparse TQWT and wavelet thresholding," *Digital Signal Processing*, vol. 153, p. 104601, Jun. 2024, doi: 10.1016/j.dsp.2024.104601.

[26] Y. Zhang, Z. Yang, X. Du, and X. Luo, "A new method for denoising underwater acoustic signals based on EEMD, correlation coefficient, permutation entropy, and Wavelet threshold denoising," *Journal of Marine Science and Application*, vol. 23, no. 1, pp. 222–237, Feb. 2024, doi: 10.1007/s11804-024-00386-6.

International Journal of Emerging Research in Engineering, Science, and Management
Vol. 5 | Issue 3 | pp. 81-96 | Jul-Sep 2026.
www.ijeresm.com | eISSN – 2583-4894
Received: 27 Apr 2026 | Revised: 29 Jul 2026 | Accepted: 12 Aug 2026 | Published: 30 Aug 2026

[27] T. Xing, X. Wang, K. Ni, and Q. Zhou, "A novel joint denoising method for hydrophone signal based on improved SGMD and WT," *Sensors*, vol. 24, no. 4, p. 1340, Feb. 2024, doi: 10.3390/s24041340.
[28] J. Li *et al.*, "WDNET : An underwater acoustic signal denoising algorithm based on Wavelet denoising and deep learning," *Internet Technology Letters*, vol. 8, no. 3, May 2025, doi: 10.1002/itl2.70022.